IAC-08-A2.4.1

CHARACTERIZATION OF THE PERFORMANCE OF AN INJECTOR FOR THE CONTROLLED GENERATION OF MICROBUBBLES

Author
Mr. Santiago Arias
Universitat Politècnica de Catalunya
Castelldefels (Barcelona), Spain
santiago.arias@upc.edu

Co-authors
Dr. Ricard González-Cinca
Universitat Politècnica de Catalunya
Castelldefels (Barcelona), Spain
ricard@fa.upc.edu

Dr. Xavier Ruiz
Universitat Rovira i Virgili and Institut d'Estudis Espacials de Catalunya,
Tarragona, Spain
josepxavier.ruiz@urv.net

Dr. Laureano Ramírez-Piscina
Universitat Politècnica de Catalunya and Institut d'Estudis Espacials de Catalunya
Barcelona, Spain
laure@fa.upc.edu

Dr. Jaume Casademunt
Universitat de Barcelona and Institut d'Estudis Espacials de Catalunya,
Barcelona, Spain
jaume.casademunt@ub.edu

ABSTRACT

We perform a characterization of a recently reported microbubble injector in conditions relevant to microgravity. Injection of bubbles is based on the generation of a slug flow in a capillary T-junction, whose operation is robust to changes in the gravity level. We address questions regarding the performance under different working regimes. In particular, we focus on the regimes found within a large range of gas and liquid injection flow rates. The injection performance is characterized by measuring bubble generation frequency. We propose curves obtained empirically for the behavior of generation frequency and crossover between regimes.

INTRODUCTION

Bubble generation and management are some of the key issues in the current research on multiphase flows for space applications [1-3]. The absence of the bouyancy force in the microgravity environment makes necessary specific configurations in order to detach bubbles from the injection device. Typical methods used are the co-flow [4], in which liquid flows parallel to the gas injection direction, and cross-flow [5], in which liquid flows perpendicularly to the gas, configurations. We propose a configuration [6,7] which is a particular case of the cross-flow one. Two flows of different phases are injected separately into a T-junction (see Fig. 1) with capillaries of the same diameter (1 mm). At the T-junction, gas bubbles are formed by the action of the liquid cross-flow. In the nominal regime of the bubble generator, capillary forces dominate over buoyancy (small Bond number[1]), and over inertial forces (small Weber number[2]). Bubble formation thus results from the competition between capillary forces and the drag due to the liquid cross-flow (note that the drag can be large even in the small flow limit when the forming bubble occupies the available cross-section of the capillary). This force balance determines bubble size and generation frequency.

---

[1] $B_o = \frac{(\rho_l - \rho_g)\, g\, \phi_c^2}{\sigma}$, ρ_l and ρ_g being the liquid and gas densities, respectively, g the gravity, ϕ_c the capillary diameter and σ the liquid surface tension.

[2] $We = \frac{\rho_l u_l^2 \phi_c}{\sigma}$, u_l being the liquid surface velocity.

We present in this paper a characterization of our injector in which larger parameter ranges than those used in [7] have been considered. This has allowed to explore different operating regimes of the injector, for which quantitative expressions for the generation frequency have been obtained.

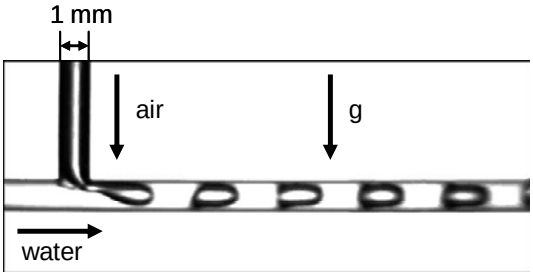

Figure 1. Detail of the T-junction inside the injector.

EXPERIMENTAL SETUP

In Fig. 2 we show a sketch of the experimental setup used in this work, which contains a test section and the air and water supply systems.

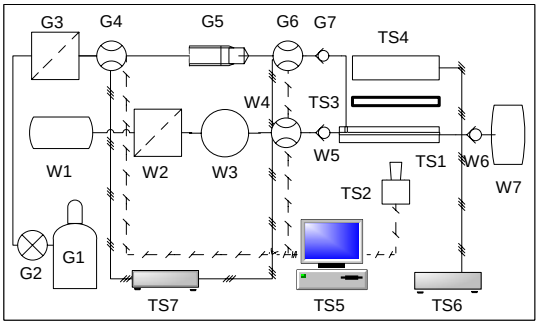

Figure 2. Experimental setup: Test Section (TS1: injector, TS2: high speed camera, TS3: diffuser, TS4: light source, TS5: server, TS6 and TS7: power supply); Air Circuit (G1: air bottle, G2: 2 stage pressure reducer, G3: air filter, G4: pressure controller, G5: chocked orifice, G6: air mass flow meter, G7: anti-return valve); Water Circuit (W1: water tank, W2: water filter, W3: water pump, W4: water mass flow meter, W5: anti-return valve, W6: anti-return valve, W7: waste bag).

Test section

The injector tested in this experiment consists of a T-junction formed by two 1 mm diameter capillaries (see Fig. 1) were the cross-flow between gas and liquid is created. Each capillary is fed by the air supply system and the water supply system, respectively. The injector is made of methacrylate with an outer square cross-section to allow recording the detachment and formation of bubbles without optical distortions due to curved surfaces. Bubble, slug and annular flows were observed with a high speed video camera with a CMOS sensor operating at 4000 frames-per-second focused at the T-junction. Rear lighting is provided by a light source with ultra bright white LED, 7000 mcd, and homogenized by a holographic diffuser sheet in order to enhance the image and the contrast between gas and liquid.

Air supply system

Synthetic and filtered air was used to avoid undesired particles. Air was driven through the capillary under constant mass flow rate with uncertainties in the measurement less than 0.50 ml/min. Mass flow rate was regulated using a chocked orifice. To such end, the pressure of the air line before the chocked orifice was regulated by a Bronkhorst Hi-Tec's air mass pressure controller/meter. The air flow rate was measured at the inlet of the capillary by a Bronkhorst Hi-Tec's air mass flow meter (F-201C9 series) under constant temperature.

Water supply system

In order to inject water into the liquid circuit and the capillary, an Ismatec MCP-Z water pump was used. Distilled and filtered water was stored in a water tank from which the water was pumped. Water flow rate was measured at the inlet of the capillary by a Bronkhorst Hi-Tec's Liquid-flow mass meter (L30 series) with uncertainties less than 0.50 ml/min. Residual air and water coming from the injector is accumulated in a residual tank.

RESULTS AND DISCUSSION

Experiments were performed under normal gravity conditions at several liquid and gas volumetric flow rates, Q_l and Q_g, respectively. Values of Q_l ranged between 1 and 60 ml/min, while Q_g ranged between 0.25 and 99 ml/min. Images were captured at 4000 fps for each chosen pair of values Q_l, Q_g. Measurement of the bubble generation frequency was carried out by an image processing software. The largest frequency achieved was around 900 bubbles per second, which was correctly resolved by the image acquisition system. Frequency aliasing was avoided in each case.

In Fig. 3 the dependence of the bubble frequency with the gas flow rate at different liquid flow rates is shown. Points correspond to slug (mainly) and bubbly flow regimes, although annular regime has also been observed at low Q_l and high Q_g. This corresponds to the parameter region in the lower left corner of the figure and explains why no frequency was measured there.

The behaviour of the bubble frequency shows two distinguishable regimes, as it was already found in [7]: a linear regime at low Q_g, and a saturation regime. Data analysed here cover a much broader region of Q_l, Q_g values than in [7], containing nearly all the pairs of flow rates that give rise to a slug flow.

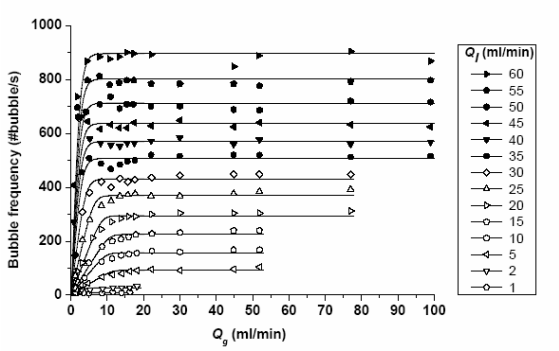

Figure 3. Bubble frequency vs. air flow rate for different liquid flow rates. *Symbols:* experimental results, *lines:* fit (Eq. (1)).

Lines in Fig. 3 correspond to the data fitting to

$$f\left(Q_g\right) = f_{sat} - a\log\left(1 + e^{-\left(Qg - x_o\right)}\right) \tag{1}$$

where x_o is the crossover point, a the slope at the linear region and $f_{sat} = x_o\, a$ being the saturation frequency. x_o is defined as the point where a line with a slope a at the origin intersects the horizontal line of the saturation region. This fitting curve is characterized by coinciding with theory [7] in the following aspects:

i) at $x << x_o$, $f(Q_g)=a\ Q_g$, which coincides with the linear behavior predicted theoretically.

ii) bubble diameter $\left(\phi_B \propto \sqrt[3]{\frac{Q_g}{f}}\right)$ does not vary at low Q_g.

Thus, Eq. (1) gives a prediction for the bubble generation frequency at given values of Q_l and Q_g which is consistent with the existing theory on the linear regime.

The saturation frequency was computed for every liquid flow rate considered, showing a linear behavior. The experimental values are shown in Fig. 4 together with the fitting line (expressed in the figure units):

$$f_{sat}\left(Q_l\right) = 15.27\,Q_l - 14.37 \tag{2}$$

Dot line in the same figure corresponds to the theoretical prediction [7]. The fitting line has a very similar slope than the one obtained in [7], in which less points were considered.

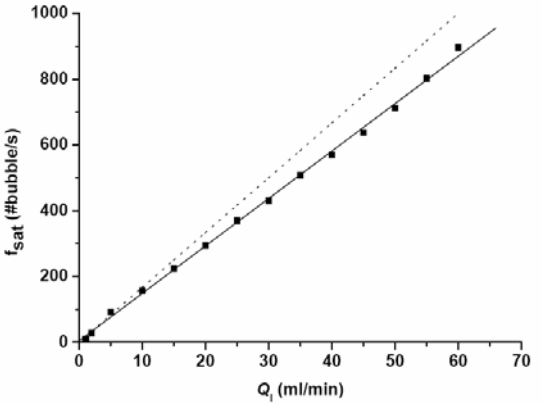

Figure 4. Saturation frequency vs. liquid flow rate. *Symbols:* experimental results, *line:* linear fit, *dot line:* theoretical prediction.

The crossover point was computed after its definition for every liquid flow rate considered (see Fig. 5). Points were fitted taking into account the following features:

i) at large values of Q_l, x_o tends to a finite value different to zero.

ii) for very low values of Q_l, f_{sat} tends to zero and a to a constant value. Thus x_o tends to zero too.

The proposed fitting curve for the crossover variation with Q_l is (Fig. 5):

$$x_o\left(Q_l\right) = d\left(b + \frac{Q_l - b}{e^{c\left(Q_L - b\right)}}\right) \tag{3}$$

with d = 3.25 (dimensionless), b = 0.51 ml/min and c = 0.12 min/ml.

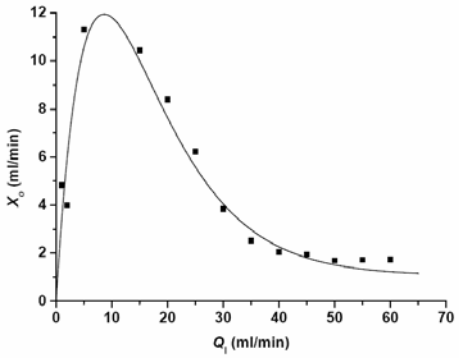

Figure 5. Crossover vs. liquid flow rate. *Symbols:* experimental results, *line:* fit.

In Fig. 6 we show the initial slope of the linear regime obtained from experimental data in Fig. 3. Combining Eqs. (2) and (3) with

$$a\left(Q_l\right) = \frac{f_{sat}\left(Q_l\right)}{x_o\left(Q_l\right)} \tag{4}$$

one obtains the fitting curve shown in Fig. 6. Both experimental points and fit show an exponential behavior at low liquid flow rates which turns to a linear tendency for higher Q_l. This linear asymptotic tendency can be expressed by (in the figure units)

$$a\left(Q_l\right) = 9.25\,Q_l - 8.70 \tag{5}$$

which is also shown in the figure.

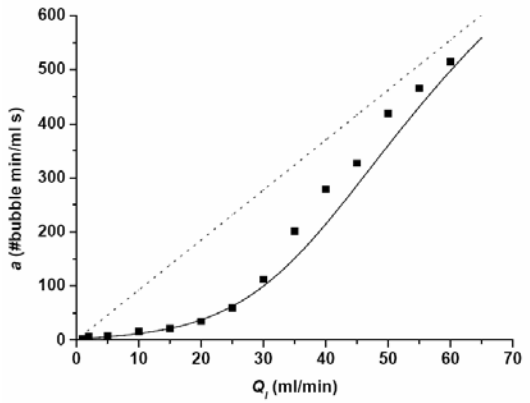

Figure 6. Initial slope of the linear regimen vs. liquid flow rate. *Symbols:* experimental results, *line:* fit, *dot line:* linear asymptotic tendency.

CONCLUSIONS

We have presented an experimental characterization of a microbubble injector for a broad region of gas and liquid flow rates, in which bubbly, slug and annular flow regimes have been observed. The slug regime, the one studied here, is characterized in our injector by a very regular bubble generation and a small dispersion in bubble size. Bubble frequency behavior at different flow rates presents a linear regime followed by a saturation state, showing a good agreement with existing theoretical predictions. A new expression for the prediction of the bubble generation frequency for given values of Q_l and Q_g has been proposed. Results obtained confirm the linear behavior of the saturation frequency with the liquid flow rate. A new expression has been proposed to predict the behavior of the crossover point between linear and saturation regimes for different liquid flow rates. The variation of the slope of the linear regime with the liquid flow rate has been found to present a linear asymptotic tendency.

It must be emphasized that the key point of this injection method is that performance in normal gravity and microgravity conditions does not show significant differences due to the small value of the Bond number. Additional advantages are reachable high bubble generation frequencies, bubble diameter of the order of the capillary and reduced bubble size dispersion.

Acknowledgements

We acknowledge financial support by Ministerio de Educación y Ciencia (Projects number ESP2006-28459-E, FIS2006-03525 and FIS2006-11452-C03-02, Spain).

REFERENCES

[1] J. McQuillen, C. Colin and J. Fabre, Ground-based gas-liquid flow research in microgravity conditions: state of knowledge, Space Forum 3, 165-203 (1998).

[2] H. Ohta, A. Baba and K. Gabriel, Review of existing research on microgravity boiling and two-phase flow, Ann. N.Y. Acad. Sci. 974, 410-417 (2002).

[3] A. A. Kulkarni and J.B. Joshi, Bubble formation and bubble rise in gas-liquid system: a review, Ind. Eng. Chem. Res. 44, 5873-5931 (2005).

[4] A. Bhunia, S.C. Pais, Y. Kamotani and I. Kim, Bubble formation in a coflow configurations in normal and reduced gravity, AIChE J. 44, 1499-1509 (1998).

[5] S.E. Forrester and C.D. Rielly, Bubble formation from cylindrical , flat and concave sections exposed to a strong liquid cross-flow, Chem. Eng. Sci. 53, 1517-1527 (1998).

[6] J. Carrera, X. Ruiz, L. Ramírez-Piscina, J. Casademunt and M. Dreyer, Generation of a monodisperse microbubble jet in microgravity, AIAA J 46, 2010-2019 (2008).

[7] S. Arias, X. Ruiz, L. Ramírez-Piscina, J. Casademunt and R. González-Cinca, Experimental study of a microchannel bubble injector for microgravity applications, accepted for publication in Microgravity Science and Technology (2008).